# The $\delta^{18}O$ of dissolved $O_2$ as a tracer of mixing and respiration in the mesopelagic ocean

Naomi Marcil Levine,[1] Michael L. Bender,[2] and Scott C. Doney[3]

Received 7 December 2007; revised 7 September 2008; accepted 21 October 2008; published 18 February 2009.

[1] The isotopic composition of dissolved oxygen in the mesopelagic ocean is a unique tracer of respiration and transport. New $\delta^{18}O$ of $O_2$ data from the tropical South Atlantic oxygen minimum zone are presented and compared to global $\delta^{18}O$ data. The $\delta^{18}O$ variability in oxygen poor waters is attributed to differences in physical and biogeochemical processes. Simple respiration-transport models show that both isopycnal diffusion and advection must be properly considered when interpreting oxygen isotope signatures along an isopycnal surface. We estimate rates of respiration and oxygen isotope fractionation for the study region using a two-dimensional (2-D) isopycnal and 1-D diapycnal model. Estimated respiration rates are consistent with previous studies. However, to account for observed $\delta^{18}O$ values at low $[O_2]$, model solutions need to invoke either very low $[O_2]$ that have not been observed in the South Atlantic or an isotope effect that is lower than values measured in the laboratory or euphotic zone.

**Citation:** Levine, N. M., M. L. Bender, and S. C. Doney (2009), The $\delta^{18}O$ of dissolved $O_2$ as a tracer of mixing and respiration in the mesopelagic ocean, *Global Biogeochem. Cycles*, *23*, GB1006, doi:10.1029/2007GB003162.

## 1. Introduction

### 1.1. Overview

[2] Respiration and transport play fundamental roles in determining the chemical and biological composition of the ocean. Respiration and remineralization add nutrients and $CO_2$ to the water column and consume $O_2$, while physical transport moves chemical signatures away from their sources (advection) and attenuates chemical gradients (diffusion). Consequently, in the subsurface aphotic (mesopelagic) ocean, the combined effect of respiration and transport is reflected in the distribution of nutrients, oxygen, carbon dioxide, and other bioactive tracers. The analysis of tracer distributions has provided information about the magnitude and variability of respiration and export rates in the mesopelagic ocean [e.g., *Feely et al.*, 2004; *Jenkins*, 1982; 1987; *Najjar et al.*, 1992; *Schlitzer*, 2002; 2004]. However, spatial variability in rates of these fundamental oceanic processes remains to be well characterized [*Buesseler et al.*, 2007].

[3] Deducing biogeochemical rates from chemical gradients would be straightforward if advection were the only mode of transport; rates could simply be calculated as the change in the concentration of a bioactive property (e.g., $O_2$) divided by the age of the water, as inferred from a time-dependent tracer such as halocarbons or tritium-$^3$He. Diffusive mixing complicates the exercise because a single water parcel contains water from different sources that have followed different trajectories. Similarly, interpretation of water age from the concentration of a time-dependent tracer is also problematic [*Doney et al.*, 1997; *Haine and Hall*, 2002]. A number of studies have examined the distribution of age tracers and respiration tracers in the presence of diffusive transport. These include *Riley*'s [1951] and *Craig*'s [1969] one-dimensional (1-D) vertical diffusion-advection model, *Haine and Hall*'s [2002] examination of the influence of diffusive mixing on the oceanic distributions of halocarbons and the implications for water mass ages, *Henning et al.*'s [2006] and *Ito and Deutsch*'s [2006] analysis of Ar supersaturation in the ocean interior as a means for estimating diapycnal mixing, and *Bender*'s [1990] and *Quay et al.*'s [1993] studies of the influence of diffusive mixing on the isotope composition of dissolved $O_2$ in seawater, the subject of this paper. These studies conclude that diffusion has a first-order influence on the distribution of tracers in the oceans, and that the process needs to be properly considered when inferring fluxes from tracer distributions. Here we argue that these studies have over estimated the role of diffusion, and that both advection and diffusion must be properly considered in order to interpret chemical tracers.

[4] Validating ocean models that invoke mixing is difficult because most properties do not show signatures that allow one to easily separate the roles of diffusion and advection. One property that strongly reflects the influence of diffusion is the $\delta^{18}O$ of dissolved $O_2$. As discussed in section 1.2, this tracer quality arises because the isotopic composition of the $O_2$ rich end-member has a dispropor-

[1]MIT-WHOI Joint Program in Oceanography/Applied Ocean Science and Engineering, Woods Hole Oceanographic Institution, Woods Hole, Massachusetts, USA.
[2]Department of Geosciences, Princeton University, Princeton, New Jersey, USA.
[3]Department of Marine Chemistry and Geochemistry, Woods Hole Oceanographic Institution, Woods Hole, Massachusetts, USA.


0886-6236/09/2007GB003162$12.00

tionate influence on the isotopic composition of a mixture. *Kroopnick and Craig* [1976], *Bender* [1990] and *Quay et al.* [1993] show that $\delta^{18}O$ of dissolved $O_2$ increases in the aphotic zone as $O_2$ is consumed through respiration. They also show that the magnitude of the increase is attenuated by diffusive mixing. The $\delta^{18}O$ of $O_2$ is a distinctive tracer in that its covariation with $O_2$ can only be simulated successfully if a model correctly describes relative rates of transport and respiration.

[5] In this paper, we present data for the $\delta^{18}O$ of $O_2$ in the thermocline of the tropical South Atlantic Ocean, the first extensive data set for this basin and for an intense $O_2$-minimum zone. We compare these data with earlier results from the Pacific [*Kroopnick*, 1987; *Quay et al.*, 1993] and Atlantic [*Kiddon*, 1993; *Kroopnick et al.*, 1972] and investigate a shift in the $\delta^{18}O/[O_2]$ relationship between oxygenated (>40% of saturation) and low oxygen (<40%) waters. We first analyze our results using a suite of diffusion-advection-reaction models [*Craig*, 1969] to characterize the interplay of physical and biological processes on the $\delta^{18}O/[O_2]$ relationship [*Bender*, 1990; *Quay et al.*, 1993]. We use the accessibility and transparency of a one-dimensional isopycnal model to analyze the sensitivity of the $\delta^{18}O/[O_2]$ relationship to advection, diffusion, respiration, and isotopic fractionation. We then use a two-dimensional isopycnal slab model to constrain rates of respiration and oxygen isotopic fractionation along an isopycnal band in the lower thermocline of the tropical South Atlantic. Finally, we investigate the importance of diapycnal processes in the oxygen minimum zone in this region. The conclusions drawn from the one-dimensional and two-dimensional model analysis are strengthened by three-dimensional model results drawn from the literature.

### 1.2. The $\delta^{18}O$ of Dissolved $O_2$ of Seawater

[6] This discussion of oxygen-18 uses the notation $\delta^{18}O$, which is defined as

$$\delta^{18}O = \left( \left[ {}^{18}O^{16}O/{}^{16}O_2 \right]_{sample} \Big/ \left[ {}^{18}O^{16}O/{}^{16}O_2 \right]_{standard} - 1 \right) \times 10^3 \quad (1)$$

where $\delta$ is given in units of per mil (‰) with respect to an air $O_2$ standard (atmospheric $O_2$ therefore has $\delta^{18}O = 0‰$ by definition).

[7] Four processes affect the concentration of dissolved $O_2$ and its $\delta^{18}O$: gas exchange, photosynthesis, respiration and mixing. In the mesopelagic ocean (the focus of this study), respiration and mixing are the processes influencing the concentration of $O_2$ and its $\delta^{18}O$. During respiration, organisms consume $^{16}O_2$ preferentially to $^{18}O^{16}O$, increasing the $\delta^{18}O$ of the remaining dissolved oxygen. Several studies have examined the magnitude of this isotope effect [*Guy et al.*, 1989; *Kiddon et al.*, 1993; *Lane and Dole*, 1956]. *Kiddon et al.* [1993] cultured a variety of organisms, ranging from bacteria to salmon, in order to determine how respiration by marine organisms affects the oxygen isotope ratio of dissolved oxygen in seawater. Results are expressed as the isotope effect, $\varepsilon$, which is defined as $\varepsilon = (1 - \alpha) \times 10^3$. The fractionation factor, $\alpha$, is the normalized ratio of $^{18}O^{16}O$ consumption to $^{16}O_2$ consumption by organisms during respiration, and $\alpha$ is defined by the following equation:

$$\frac{d\left[{}^{18}O^{16}O\right]/dt}{d\left[{}^{16}O^{16}O\right]/dt} = \frac{\left[{}^{18}O^{16}O\right]}{\left[{}^{16}O^{16}O\right]} \times \alpha \quad (2)$$

[8] *Kiddon et al.* [1993] found an average isotope effect of 20 ± 3‰ ($\alpha$ = 0.980) for the respiration of small unicellular marine organisms, including autotrophs and heterotrophs. They suggested that the average isotope effect measured for heterotrophic bacteria, 18.6 ± 0.5‰ ($\alpha$ = 0.981), is a good approximation for respiration occurring in the dark ocean. This value is validated by subsequent studies in culture [*Guy et al.*, 1989; *Helman et al.*, 2005] and in ocean surface waters [*Hendricks et al.*, 2005; *Quay et al.*, 1993], and appears to be well constrained. It is important to note that nitrification also affects the isotopic signature of oxygen. Currently, the nitrification fractionation factor is not known and so, similar to previous studies, we assume that nitrification has a similar fractionation factor to respiration.

[9] In the absence of mixing, the isotopic fractionation of dissolved $O_2$ during consumption is given by the Rayleigh equation, the integrated solution to equation (2) using equation (1) to express the results in $\delta^{18}O$ notation:

$$\delta^{18}O = 1000 \times \left( f^{(\alpha-1)} - 1 \right) \quad (3)$$

where $f$ is $[{}^{16}O_2]/[{}^{16}O_2]_{sat}$ and $\alpha$ is the isotope fractionation factor. Dissolved oxygen is assumed to be initially in equilibrium with the atmosphere. Thus, initially $[O_2] = [O_2]_{sat}$ and $\delta^{18}O$ is equal to the equilibrium fractionation between air and dissolved $O_2$ (0.75‰), when the standard is atmospheric $O_2$. In the following discussion, we equate $[O_2]$ and $[{}^{16}O_2]$. This simplification introduces no significant error in the $\delta^{18}O$ versus $[O_2]/[O_2]_{sat}$ relationship because of the small abundance of $^{18}O^{16}O$. Figure 1 shows two Rayleigh (closed system) fractionation curves for dissolved oxygen calculated using two different $\alpha$ values. Also plotted in Figure 1 are $\delta^{18}O$ of $O_2$ values for water samples from the Pacific [*Kroopnick*, 1987], South Atlantic [this study and *Kiddon*, 1993], North Atlantic [*Kroopnick et al.*, 1972], and subarctic Pacific [*Quay et al.*, 1993]. All $\delta^{18}O$ data fall significantly below the Rayleigh curves for $\alpha$ = 0.981. The Rayleigh curve for $\alpha$ = 0.990 falls closest to the data but does not correctly reproduce the curvature in the data.

[10] Mixing also affects the isotopic composition of dissolved $O_2$ [*Bender*, 1990; *Kroopnick and Craig*, 1976; *Quay et al.*, 1993]. While $[O_2]$ of a mixture is determined only by the fraction-weighted concentration of the end-members, $\delta^{18}O$ is determined both by the $\delta^{18}O$ and by the $[O_2]$ concentrations of the end-members. Thus, $\delta^{18}O$ always changes nonlinearly with the fraction of end-members in the mix. Furthermore, the relation between $\delta^{18}O$ and $[O_2]/[O_2]_{sat}$ depends on the interaction between mixing and respiration. Consider two end-members falling on a single Rayleigh curve, one of low $[O_2]/[O_2]_{sat}$ and high $\delta^{18}O$ and the other of high $[O_2]/[O_2]_{sat}$ and low $\delta^{18}O$. Mixing of such

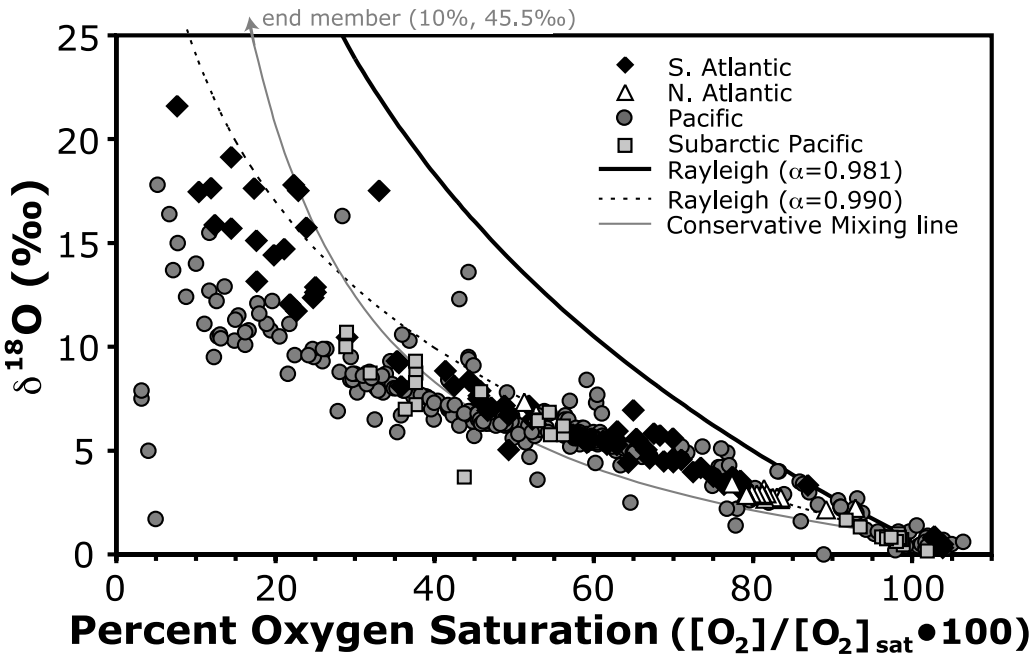


**Figure 1.** Rayleigh curves (closed system $O_2$ consumption), mixing lines, and $\delta^{18}$O of $O_2$ data. The Rayleigh curves are calculated using $\alpha = 0.981$ and 0.990, corresponding to isotope effects of 19‰ and 10‰, respectively. The gray line is a two-end-member mixing line using endpoints falling on the Rayleigh curve for $\alpha = 0.981$. The endpoints correspond to $O_2$ at equilibrium with air and $[O_2]/[O_2]_{sat} = 0.10$. The symbols represent measured $\delta^{18}$O of dissolved $O_2$ from four data sets: the South Atlantic SAVE-2 data set (this study and *Kiddon* [1993]), the North Atlantic GEOSECS II data set [*Kroopnick et al.*, 1972], the Pacific GEOSECS data set [*Kroopnick*, 1987], and subarctic Pacific data set [*Quay et al.*, 1993].

end-members always yields water with a $\delta^{18}$O value that falls below the Rayleigh $\delta^{18}$O value for the $[O_2]$ of the mixture. This is because the isotopic composition of the mixture is dominated by the high-$O_2$, low-$\delta^{18}$O end-member. An example of this is shown in Figure 1 where water at 10% oxygen saturation and a $\delta^{18}$O value of 45.5‰ (a point chosen from the $\alpha = 0.981$ Rayleigh curve) is mixed with water at 100% saturation and a $\delta^{18}$O value of 0.75‰. At intermediate values of $[O_2]/[O_2]_{sat}$, the resulting mixing curve falls far below the Raleigh fractionation curve for $\alpha = 0.981$, by 10‰ or more. Mixing curves, such as the ones shown in Figure 1, provide a qualitative explanation for the systematic difference between the observed curvature of $\delta^{18}$O versus percent $O_2$ saturation and the Rayleigh fractionation curve.

[11] Motivated by its unique tracer quality, several workers have used ocean models of varying complexity to quantitatively examine variations of the $\delta^{18}$O of $O_2$ in the oceans [*Bender*, 1990; *Kroopnick and Craig*, 1976; *Maier-Reimer*, 1993; *Quay et al.*, 1993]. Their results show that it is possible to reproduce the observed relationship between $\delta^{18}$O of $O_2$ and the degree of $O_2$ saturation in the oceans. However, all studies require one or more of the following conditions: the respiratory $^{18}$O isotope effect is about 10‰ ($\alpha = 0.990$) rather than 19‰, diffusion rather than advection dominates isopycnal transport, diapycnal mixing is the dominant mode of transport in the euphotic zone, or an end-member that is almost completely depleted in $O_2$. In this paper, we present new data for the distribution of $\delta^{18}$O of $O_2$ in the tropical South Atlantic, a region that appears to lack extreme values of $O_2$ depletion. We use 1-D and 2-D models of ocean mixing to examine these results and data from previous studies. We then consider whether or not it is possible to quantitatively explain the distribution of $\delta^{18}$O of $O_2$ by invoking known oceanographic processes.

## 2. South Atlantic Ventilation Experiment Samples

### 2.1. Description

[12] The 81 samples analyzed in this paper were collected between 18.9°S, 37.8°W and 10.2°S, 12.6°E in January 1988 on Leg 2 of the South Atlantic Ventilation Experiment (SAVE-2) [*South Atlantic Ventilation Experiment*, 1992]. This east-west transect cuts across the northern portion of the South Atlantic gyre and runs through the South Atlantic oxygen minimum zone found off the coast of Africa. This strong oxygen minimum zone is thought to result from a combination of slow ventilation rates and high respiration rates [*Brea et al.*, 2004; *Broecker et al.*, 1991; *Chapman and Shannon*, 1987]. The samples were collected at 15 stations at a range of depths focusing on the upper 1000 m. An additional 16 samples from SAVE-2 were collected and analyzed by J.A. Kiddon at the University of Rhode Island

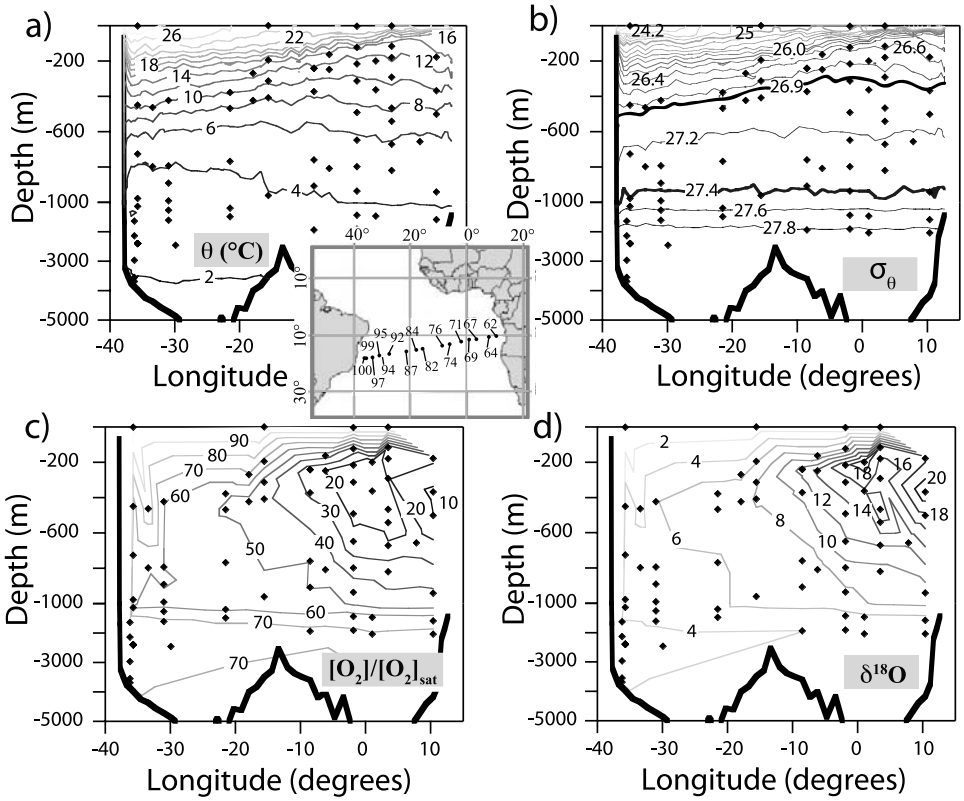


**Figure 2.** Contour diagrams of properties on Leg 2 of the South Atlantic Ventilation Experiment (note the change in depth scale at 1000 m). Endpoints of the section are 18.9°S, 37.8°W and 10.2°S, 12.6°E. The inset in Figure 2a shows the location of the 16 stations at which samples were collected. The sample locations are represented in the sections by the black diamonds. The seafloor is represented by the thick black line. Figure 2a plots the isotherms for the transect using a contour interval of 2°C. Figure 2b plots the isopycnal surfaces (potential density) for the transect using a contour interval of 0.2 $\sigma_\theta$ units. The thick lines denote the approximate isopycnal band used in the model analysis ($26.90 \leq \sigma_\theta < 27.4$). Figure 2c plots the oxygen saturation ($[O_2]/[O_2]_{sat} \times 100$) for the 77 SAVE-2 samples with a contour interval of 10% saturation. Figure 2d plots the $\delta^{18}$O of dissolved $O_2$ for the 77 SAVE-2 samples with a contour interval of 2‰.

(the sampling procedure and data are presented in *Kiddon* [1993]). The latitude and longitude of the stations and the location of the SAVE-2 samples (this paper) in relationship to potential temperature, potential density and oxygen saturation profiles are shown in Figure 2.

### 2.2. Method

[13] During SAVE-2, a sampling package containing a CTD and 24 Niskin bottles was used to collect water samples for hydrographic measurements: temperature, salinity, $[O_2]$, nutrient and chlorofluorocarbon (CFC) concentrations, etc. At the chosen stations, approximately 100 mL of water from selected depths was transferred from the Niskin bottles to BOD bottles (glass bottles with ground glass joints). The BOD bottles were then stored in the dark for up to an hour. The dissolved gases were extracted from the water sample and collected in breakseal glass vials using the method described by *Bender and Grande* [1987].

[14] The oxygen isotopic composition of the samples was analyzed at Princeton University, during 2002–2003, using mass spectrometry. The breakseal vials are scored and inserted into a breaker connected to a vacuum line evacuated to $<10^{-3}$ torr. The breakseal vials are cooled to −70°C for 20–30 min to freeze out water vapor. Once the vial is broken, the gas is passed through a trap immersed in liquid nitrogen to remove $CO_2$ and any remaining water vapor. Finally, the sample is quantitatively condensed into a stainless steel sample tube immersed in liquid helium. After collection, the stainless steel tubes are allowed to reequilibrate to room temperature for an hour. Samples are analyzed with a ThermoFinnigan Delta Plus XP dual inlet mass spectrometer. The $\delta^{18}$O of $O_2$, $\delta^{15}$N of $N_2$, $\delta$Ar/$O_2$, $\delta N_2/O_2$ and $\delta$Ar/$N_2$ ratios of each sample are measured simultaneously relative to an air standard.

[15] As a test of sample integrity, we use $\delta$Ar/$O_2$ values to calculate the $[O_2]$ of samples analyzed at Princeton assum-

ing the samples to be saturated with respect to Ar. Solubilites are calculated from *Weiss* [1970]. The measured $[O_2]$ deviate from SAVE-2 Winkler titration values by >9% in only four samples; these results were discarded. We perform the Student *t* test, and the remaining $[O_2]$ values calculated at Princeton are not significantly different (95% confidence interval) from the Winkler titration data. Excluding the four anomalous samples, we calculate a negligible negative bias of −0.07%. There is structure in the residuals; samples in the upper 600 m have a negative bias (−1.44%) whereas samples from depths greater than 600 m have a small positive bias (+0.95%). Since the $[O_2]$ calculated from the mass spectrometer measurements assumes that Ar is at saturation, a small Ar supersaturation at shallow depths could explain why we underestimate $O_2$ in the upper water column. Similarly, a slight undersaturation of Ar at greater depth could explain the why we overestimate $O_2$ in these samples. This result is consistent with the calculations of *Ito and Deutsch* [2006], whose modeling of Ar saturation states indicates that significant Ar supersaturation occurs in the upper 500 m, particularly in the tropics, and significant undersaturation occurs in deep waters and regions with a well ventilated thermocline. The root mean squared deviation between the calculated $[O_2]$ and the Winkler $[O_2]$ is 2.64 $\mu$mol/kg or ±0.9%. The interpretation of this comparison is that our stored samples preserve the dissolved $O_2$ of the original seawater.

[16] When measuring $\delta^{18}O$ with our method, a correction must be made for the ratio of $N_2$ to $O_2$ present in the sample [*Kiddon*, 1993; *Sowers et al.*, 1989]. The magnitude of this correction appears to be dependent on the mass spectrometer and its tuning. This correction is measured by running a series of calibration samples, with identical isotopic compositions but with varying $[N_2]/[O_2]$ ratios, against an air standard. Calibration samples have $\delta N_2/O_2$ values spanning the entire sample range from −515‰ to +5250‰ with respect to air, which corresponds to conditions from about 100% to 10% of $O_2$ saturation. The relationship between $\delta^{18}O$ and $\delta N_2/O_2$ for the calibration samples is linear throughout this range.

[17] We assess the procedural error by expanding aliquots of the air standard into breakseal glass vials, sealing them, and analyzing them as samples. The measured $\delta^{18}O$ for eight of these samples is $-0.08 \pm 0.03$‰ ($1\sigma$). The standard deviation from the mean of six replicate SAVE-2 samples collected in duplicate is ±0.13‰ for $\delta N_2/O_2$ and ±0.08‰ for $\delta^{18}O$. These errors are smaller than the symbols used to represent the data points and so are not shown in the figures.

### 2.3. SAVE-2 $O_2$ and $\delta^{18}O$ Distributions

[18] The hydrographic properties along SAVE-2 are summarized in Figure 2. The station number, location, depth, potential density ($\sigma_\theta$), oxygen concentration ($\mu$mol/kg), percent oxygen saturation ($[O_2]/[O_2]_{sat} \times 100$), and $\delta^{18}O$ of dissolved $O_2$ (‰) for the 77 SAVE-2 samples we analyzed are provided in the supplementary material (Table S1).[1] Four samples excluded on the basis of anomalous $[O_2]$ relative to the SAVE-2 Winkler $[O_2]$ data, discussed in section 2.2, are not presented. The measured $\delta^{18}O$ values are shown as a contour plot in Figure 2d. The region of high $\delta^{18}O$ in the thermocline on the eastern part of the basin corresponds with the intense oxygen minimum zone shown in Figure 2c. The $\delta^{18}O$ of dissolved $O_2$ data for the 77 SAVE-2 samples are plotted versus $[O_2]/[O_2]_{sat} \times 100$ in Figures 1 and 4d. The $\delta^{18}O$ values increase approximately linearly as $[O_2]/[O_2]_{sat}$ decreases from 100% to 40% saturation. As oxygen values decrease below 40% saturation, the $\delta^{18}O$ values rise at an increasing rate but never reach values predicted by the Rayleigh fractionation curve, given typical $\alpha$ values for marine organisms ($\alpha = 0.978-0.986$, Kiddon et al. 1993). All SAVE-2 samples with oxygen saturation values less than 40% represent oxygen minimum zone samples and are located above 1000 m and east of 9°W (Figure 2c). In the oxygen minimum zone, samples with the same value of $[O_2]/[O_2]_{sat}$ have $\delta^{18}O$ values that vary by as much as 7‰. At low $[O_2]$, SAVE-2 samples on shallower isopycnals tend to have higher $\delta^{18}O$ values than samples on deeper isopycnals with the same $[O_2]/[O_2]_{sat}$. The different $\delta^{18}O$ signatures of the isopycnal bands might be explained by different rates of respiration, mixing and advection occurring along the isopycnal surfaces (e.g., Figure 3). We explore this possibility further by determining the effect of relative rates of these properties on the $\delta^{18}O/[O_2]$ relationship (discussed in section 3.2).

[19] Figure 1 presents the South Atlantic [this study and *Kiddon*, 1993] $\delta^{18}O$ data in the context of other available ocean $\delta^{18}O$ of $O_2$ data from the Pacific [*Kroopnick*, 1987; *Quay et al.*, 1993], and North Atlantic [*Kroopnick et al.*, 1972]. Despite the wide range of mixing and respiration histories represented by the data shown in Figure 1, there is a uniform relationship across the basins between $\delta^{18}O$ of $O_2$ and $[O_2]/[O_2]_{sat}$ for all samples with $[O_2]$ greater than 40% of saturation. We suggest that this compact relationship results from the insensitivity of the $\delta^{18}O$ signature to mixing at high $[O_2]$, as well a similarity in the patterns of mixing and respiration experienced by the oxygenated water samples.

[20] At low $O_2$ levels (<40% of saturation), the $\delta^{18}O$ of global samples for a particular $[O_2]/[O_2]_{sat}$ value vary by up to 10‰. The largest variation occurs between the Pacific and South Atlantic samples, which may be attributed to the different pathways by which the low-$[O_2]$, high-$\delta^{18}O$ waters were formed. The high $\delta^{18}O$ of $O_2$ values in the South Atlantic are associated with the thermocline oxygen minimum zone (<1000 m) resulting from advective transport through the gyre, slow ventilation, and high respiration rates. On the other hand, the majority of low $[O_2]$ and corresponding high-$\delta^{18}O$ waters in Kroopnick's Pacific data set are located at greater depths (>1000 m). These waters evolve through the mixing of different water masses that have experienced slow respiration rates over extended periods of time [*Key et al.*, 2002]. Simple 1-D model results, described in section 3.2, indicate that slow ventilation and high respiration rates can yield very high $\delta^{18}O$ values. Alternatively, increased ventilation and lower respiration rates yield lower $\delta^{18}O$ values (see discussion in sections 3 and 4). The variations in the $\delta^{18}O/[O_2]$ relationship observed

[1] Auxiliary materials are available in the HTML. doi:10.1029/2007GB003162.

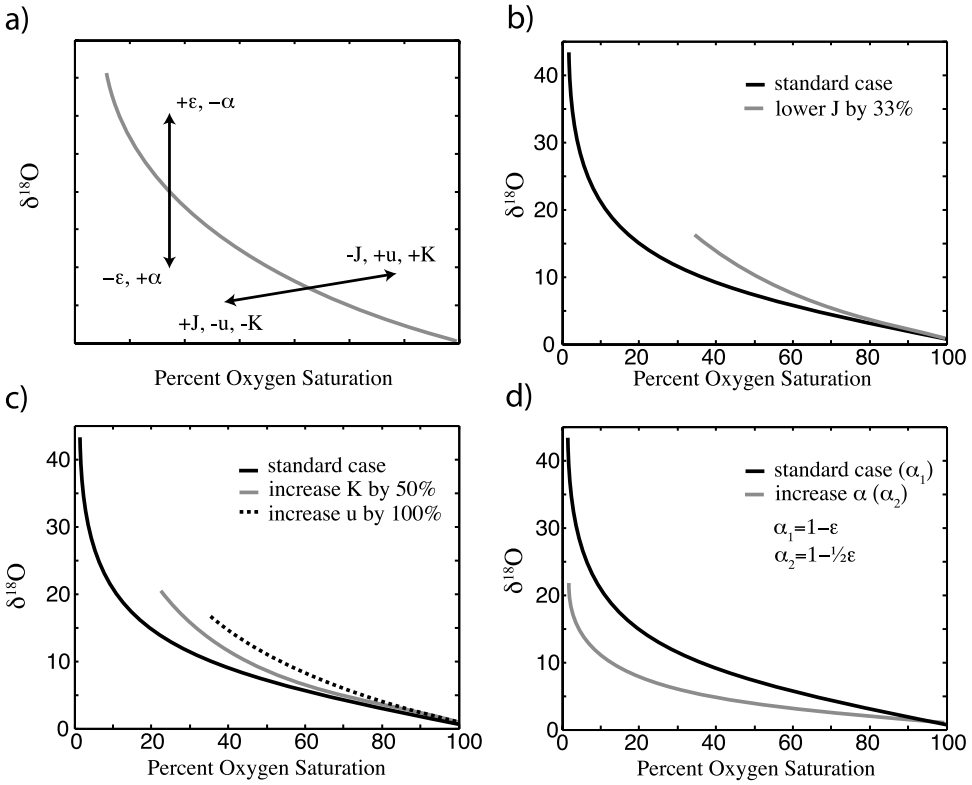


**Figure 3.** One-dimensional isopycnal model sensitivity study. Figure 3a displays the effect of advection ($u$), diffusion ($K$), respiration ($J$), and isotopic fractionation ($\alpha$, $\varepsilon$) on the $\delta^{18}O/[O_2]$ relationship. Increased respiration ($+J$), decreased advection ($-u$), and decreased diffusion ($-K$) act to decrease the minimum $[O_2]/[O_2]_{sat}$ and thus $\delta^{18}O$ via mixing. The model displays a high degree of sensitivity to the isotopic fractionation factor ($\alpha$) with an increase in $\alpha$ (decrease in $\varepsilon$) resulting in a significant change in both maximum $\delta^{18}O$ value and in the curvature of the $\delta^{18}O/[O_2]$ relationship. Figures 3b, 3c, and 3d display examples of model output for a range of parameters relative to a standard case with a Peclet number of 2 ($\alpha = 0.982$, $J = 1.1$ $\mu$mol/kg, $K = 1000$ m$^2$/s, $u = 0.0004$ m/s). Figure 3b shows the effect of decreasing $J$ by 33%. Figure 3c displays the result of doubling advection and increasing diffusion by 50%. Figure 3d shows the effect of halving the isotope effect, $\varepsilon$, where $\alpha = 1 - \varepsilon$.

in different types of low-oxygen waters demonstrates that additional $\delta^{18}O$ of $O_2$ data, interpreted in the context of models, can further illuminate the evolution of tracer fields in oxygen minimum zones.

## 3. Understanding the $\delta^{18}O$ Signal

[21] As discussed in sections 1.2 and 2.3, the isotopic signature of $O_2$ is controlled by isotopic fractionation and the relative rates of ventilation and remineralization experienced by a water parcel. Advection-diffusion-reaction models can be used to deconvolve the $\delta^{18}O/[O_2]$ relationship and elucidate these important processes. One-dimensional models have been widely used to interpret tracer distributions and to estimate rates of physical and biological processes [e.g., *Bender*, 1990; *Craig*, 1969; *Jenkins*, 1988; *Robbins et al.*, 2000]. Here we use a 1-D isopycnal model to examine the sensitivity of the $O_2$ isotopic signature to advection, diffusion, respiration and respiratory fractionation. We then interpret the SAVE-2 data using a 2-D isopycnal slab model. Finally, we assess the importance of diapycnal processes with a 1-D diffusion-reaction model.

### 3.1. Advection-Diffusion-Reaction Model Description

[22] The models presented here invoke advection, eddy diffusion, and tracer consumption ($O_2$ consumption). The general equation for the change of a tracer concentration ($C$) with respect to time in one dimension can be written as

$$\frac{\partial C}{\partial t} = K\frac{\partial^2 C}{\partial x^2} - u\frac{\partial C}{\partial x} - J \tag{4}$$

where $K$ is an eddy diffusion coefficient in m$^2$/s, $u$ is an advection term in m/s, $J$ is a consumption or production term, and $x$ is the distance in meters along an isopycnal surface or across isopycnal surfaces (diapycnal or approximately vertical). For the 2-D case, equation (4) is expanded to

$$\frac{\partial C}{\partial t} = K_x\frac{\partial^2 C}{\partial x^2} + K_y\frac{\partial^2 C}{\partial y^2} - u\frac{\partial C}{\partial x} - v\frac{\partial C}{\partial y} - J \tag{5}$$

[23] For the 1-D models, $x$ is calculated either as the distance along a line between the western and eastern most data point of an isopycnal surface (isopycnal model) or as the distance along a vertical line between the upper and lower bounds of the $O_2$ minimum zone (diapycnal model). For simplicity, the 2-D model uses a basin width ($x$) of 3000 km and a length ($y$) of 6000 km. We discretize equations (4) and (5) using the forward upwind differencing method with a d$x$ value of $5 \times 10^4$ m for the isopycnal model, 48 m for the diapycnal model, and $6 \times 10^4$ m for the 2-D model (d$x$ = d$y$). We use a time step (d$t$) of $1 \times 10^6$ s ($\sim$0.03 years) for both the isopycnal and diapycnal models. For the 2-D model, d$t$ is calculated on the basis of the model parameters in order to assure stability.

[24] The models are run using two forms of equations (4) or (5), one for $[O_2]$ or $[^{16}O_2]$ and one for $[^{18}O^{16}O]$. The consumption term, $J$, is given in units of mmol/m$^3$/s ($J < 0$). To facilitate comparison with previous studies, we convert our $J$ values using a fixed seawater density to the more conventional units of $\mu$mol/kg/a. For $[O_2]$, the consumption rate ($J_{16,16}$) is independent of concentration and depth and so is constant for all model boxes. However, the consumption rate of $^{18}O^{16}O$ ($J_{18,16}$) is dependent on the $^{18}O^{16}O/^{16}O_2$ of the dissolved $O_2$, and is written as

$$J_{18,16} = J_{16,16} \times \alpha \times \left[^{18}O^{16}O\right] / \left[^{16}O_2\right] \quad (6)$$

where $\alpha$ is the fractionation factor.

[25] All models are initialized with a uniform tracer concentration, $C_{initial}$, which is determined from the tracer data. The models are then integrated forward in time until the model converges on a steady state solution. For the 1-D isopycnal model, the upstream boundary condition ($x = 0$) is fixed at $C_{initial}$ and the downstream boundary condition (eastern boundary) is treated as a wall; therefore the last model box exchanges only with the adjacent box on the upstream side. The tracer concentrations at the upper and lower boundaries of the diapycnal model are fixed on the basis of tracer data.

[26] The 2-D isopycnal slab model contains two gyres: an anticyclonic gyre to the south and a cyclonic gyre to the north (Figure 4a). The 2-D model's advective geometry attempts to mimic the circulation observed in the South Atlantic with an anticyclonic gyre between 15°S and 40°S composed of the Brazil Current, South Atlantic Current and Benguela Current, and the cylonic Angola gyre between 5°S and 15°S [*Stramma and England*, 1999]. In the model, both gyres have intensified western boundary currents. To facilitate communication between the two gyres, a highly diffusive region (9000 m$^2$/s) is added to the western portion of the boundary between the gyres. The southern boundary of the model is fixed at atmospheric levels (100% $O_2$ saturation, $\delta^{18}O$ value of 0.75‰) and no exchange is permitted across the northern, eastern and western boundaries.

### 3.2. Model Sensitivity Analysis

[27] We use the 1-D isopycnal model to conduct a series of sensitivity tests to determine the effects of model parameters on the $\delta^{18}O/[O_2]$ relationship. The results of this exercise are summarized in Figure 3a. As expected, the minimum value of $[O_2]/[O_2]_{sat}$ decreases with higher respiration rates (+$J$, Figure 3b). Advection and diffusion counteract respiration with decreased ventilation ($-u$, $-K$) resulting in lower minimum $[O_2]/[O_2]_{sat}$ values (Figure 3c). The relative importance of advection and diffusion in a region are determined by the Peclet number (Pe = $uL/K$, where $u$ is the advection term, $L$ is the basin length scale, and $K$ is the eddy diffusion coefficient). Previous studies [e.g., *Jenkins*, 1998; *Robbins et al.*, 2000] have shown that open ocean Peclet numbers are fairly low indicating that eddy diffusion and large-scale advection have the same order of importance on tracer distributions particularly away from outcrop regions. Here we use a 1-D model Peclet number of 2 chosen from the literature [*Robbins et al.*, 2000] which argues for approximately equal importance of advection and diffusion. Including advection allows the 1-D isopycnal model to reproduce the linear relationship between $\delta^{18}O$ and $O_2$ observed in the global samples at high $O_2$ saturations, >40% saturation (Figure 1), while diffusion allows the model to reproduce the curvature of the $\delta^{18}O/[O_2]$ relationship particularly at low $O_2$ saturations.

[28] The advection-diffusion-reaction models are sensitive to changes in the fractionation factor ($\alpha$). For example, for a fixed oxygen saturation of 20%, increasing the model $\alpha$ from 0.982 to 0.991 (50% reduction in $\varepsilon$, where $\alpha = 1 - \varepsilon$) decreases model $\delta^{18}O$ by 50% from 25.0‰ to 12.8‰ (Figure 3d). This sensitivity highlights the need for well-constrained isotopic fractionation factors when interpreting the oxygen isotopic signature.

[29] For simplicity, $J$ is treated as a spatially uniform constant in each simulation. We perform sensitivity tests to determine the impact of spatially varying $J$ in the isopycnal and diapycnal 1-D models. The models are run using a scaled Martin curve [*Martin et al.*, 1987] calculated using the change in depth along the transect. This produces a variable respiration rate that changes by 600% over the model domain. Both the isopycnal and diapycnal models produced the same $\delta^{18}O$ to $O_2$ relationship using a spatially varying $J$ as using a constant $J$ equal to the mean of the scaled Martin curve. From this we conclude that, for our 1-D models, a constant $J$ value is also a good approximation for the mean consumption rate across the model surface.

### 3.3. Two-Dimensional Model Results

[30] The 2-D isopycnal slab model is used to analyze the $[O_2]$ and $\delta^{18}O$ values for a lower-thermocline isopycnal band along the SAVE-2 transect, $26.90 \leq \sigma_\theta < 27.4$. Using an average advective velocity of 0.01 m/s (calculated as the mean velocity vector for the eastern half of the model basin) and a diffusion coefficient of 1000 m$^2$/s, the model estimates the average consumption along the transect to be approximately 2.9 $\mu$mol/kg/a (2.85 $\mu$mol/kg/a to be exact). With a fractionation factor of 0.981, the 2-D model reproduces the $\delta^{18}O$ of $O_2$ signature observed in the data (Figure 4). However, the model requires an extremely low $[O_2]/[O_2]_{sat}$ (2.08%) and extremely high $\delta^{18}O$ (50.3‰) end-member in order to reproduce the observed $\delta^{18}O/[O_2]$ relationship. For comparison, the low-$O_2$ end-member of the data set (SAVE-2) has a $\delta^{18}O$ = 21.6‰ with an oxygen saturation of 7.6%.

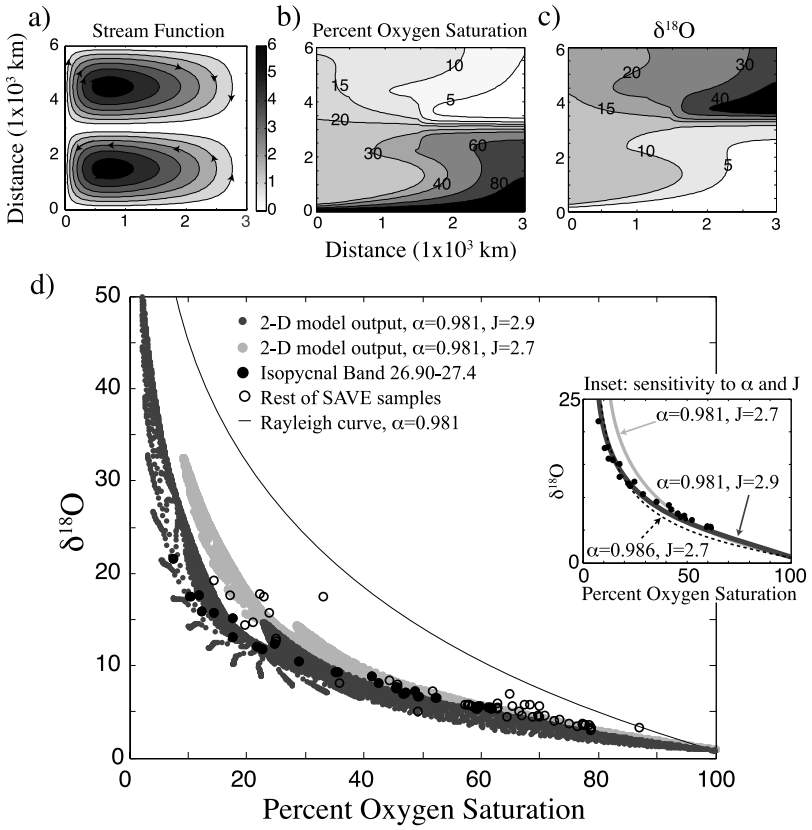


**Figure 4.** Two-dimensional isopycnal slab model solution and SAVE $[O_2]$ and $\delta^{18}$O data. Figure 4a displays the advection geometry used in the 2-D model. Figures 4b and 4c plot model percent of $O_2$ saturation and model $\delta^{18}$O values for $J = 2.9$ $\mu$mol/kg and $\alpha = 0.981$, respectively. Figure 4d plots $\delta^{18}$O of $O_2$ versus percent oxygen saturation for the SAVE data and two 2-D model solution, $J = 2.9$ $\mu$mol/kg and $J = 2.7$ $\mu$mol/kg ($\alpha = 0.981$, $K = 1000$ m$^2$/s, and average advection = 0.01 m/s for both cases). Samples falling on the lower-thermocline isopycnal band analyzed using the 2-D model, $26.90 \leq \sigma_\theta < 27.4$ (solid black circles), are distinguished from the rest of the samples (open circles). The closed system Rayleigh fraction curve ($\alpha = 0.981$) is included in Figure 4d for reference. The inset in Figure 4d shows the 2-D model sensitivity to $\alpha$. Displayed are model output for two different $\alpha$ values, 0.981 and 0.986, and two different $J$ values, $J = 2.9$ $\mu$mol/kg and 2.7 $\mu$mol/kg (for clarity, best fit lines are plotted instead of model output).

[31] The 2-D model shows the same qualitative sensitivity to model parameters as the 1-D isopycnal model (discussed in section 3.2 and shown in Figure 3a). The geometry of the 2-D model results in a low effective Peclet number, indicating approximately equal importance of diffusion and advection in determining the oxygen isotopic signature. Decreasing the respiration rate ($J$) eliminates the low-$O_2$, high-$\delta^{18}$O end-member (Figure 4d), but results in model $\delta^{18}$O/$[O_2]$ output that falls above the data particularly at low $O_2$ saturations when $\alpha = 0.981$. Decreasing the isotope effect (increasing $\alpha$) acts to depress the $\delta^{18}$O/$[O_2]$ relationship allowing the 2-D model to fit the observations without the low-$O_2$ end-member (Figure 4d, inset). However, increasing $\alpha$ changes the curvature of the model output causing the model $\delta^{18}$O/$[O_2]$ values to fall below the observations at middle and high $O_2$ saturations.

### 3.4. Diapycnal Model Results

[32] One dimensional models can be applied either horizontally along isopycnal surfaces or vertically across isopycnal surfaces. Diapycnal processes are thought to play a minor role, relative to isopycnal advection and diffusion, in supplying $O_2$ to the well ventilated thermocline of subtropical gyres [*Ledwell et al.*, 1993]. However, this finding may not hold for tropical oxygen minimum zones, where direct ventilation is reduced and diapycnal concentration gradients are sharper. A simple scaling argument of the implied $O_2$ consumption needed to balance diapycnal diffusion in the South Atlantic $O_2$ minimum zone indicates that the diapycnal oxygen convergence could significantly contribute to the total $O_2$ consumption in the study region.

[33] The one-dimensional diapycnal model is used to analyze $[O_2]$ and $\delta^{18}$O data in the oxygen minimum zone (292–819 m) between 1.9°W and 10.4°E, as the effects of

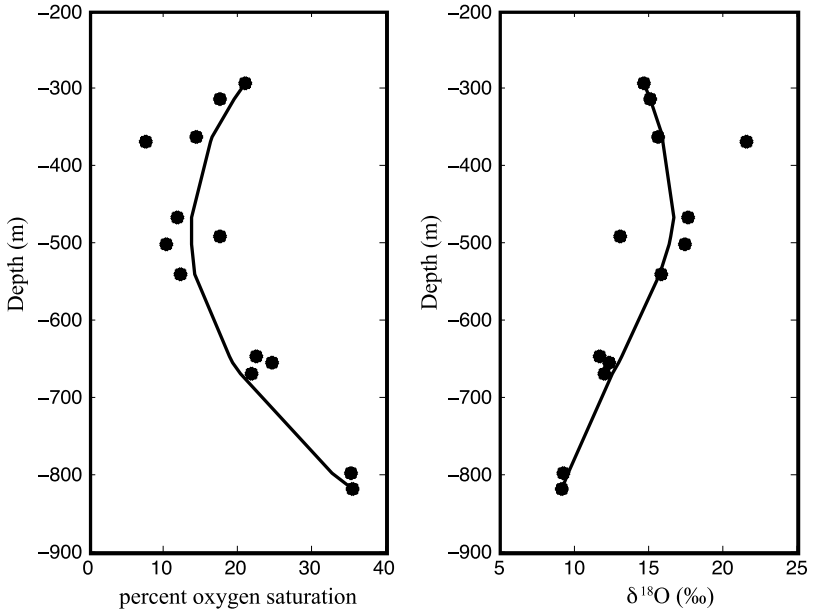


**Figure 5.** Best fit diapycnal model solution to SAVE $[O_2]$ and $\delta^{18}O$ data from the oxygen minimum zone (1.9°W to 10.4°E). The left-hand panel plots percent oxygen saturation versus depth for the SAVE data and the best fit model solution. The right-hand panel plots $\delta^{18}O$ of $O_2$ versus depth for the SAVE data and the best fit model solution. The best fit model parameters are $\alpha = 0.992$ and $J = 0.31$ $\mu$mol/kg/a ($K = 1 \times 10^{-5}$ m$^2$/s, $u = 0$ m/s).

diapycnal diffusion are expected to be greatest in this region. The upper and lower boundaries are fixed from observations at $[O_2]/[O_2]_{sat} = 21.1\%$ and $\delta^{18}O = 14.7‰$, and $[O_2]/[O_2]_{sat} = 35.6\%$ and $\delta^{18}O = 9.2‰$, for 292 m and 819 m, respectively. With a diffusion coefficient of $1 \times 10^{-5}$ m$^2$/s and zero vertical advection, the diapycnal model best fits the data using a respiration rate of 0.31 $\mu$mol/kg/a and a fractionation factor of 0.992 (Figure 5). This isotope effect is significantly lower (higher $\alpha$) than those observed in laboratory experiments (average 0.981). This is similar to the 2-D case in which the model could fit the data without a low-$O_2$ end-member by decreasing the isotope effect. This result is discussed in detail in section 4.

## 4. Modeling Discussion

[34] Using the two-dimensional isopycnal slab model we estimate the average respiration rate along the lower-thermocline isopycnal band ($26.90 \leq \sigma_\theta < 27.4$, ~400–800 m) to be approximately 2.9 $\mu$mol $O_2$/kg/a. In the oxygen minimum zone, we estimate that diapycnal convergence for low-eddy diffusivities (e.g., consistent with *Ledwell et al.* [1993]) requires a consumption rate of 0.31 $\mu$mol $O_2$/kg/a. In steady state, both isopycnal and diapycnal diffusion cause a physical convergence of oxygen that needs to be balanced by a biological sink. Therefore, we combine the isopycnal and diapycnal rates to estimate a total oxygen consumption rate of 3.2 $\mu$mol $O_2$/kg/a. These results are consistent with previous estimates of oxygen consumption rates. *Jenkins* [1987] estimates oxygen consumption rates between 1.1 and 7.6 $\mu$mol $O_2$/kg/a for $\sigma_\theta = 27.15$ to 27.72 (609–1263 m) in the North Atlantic Beta Triangle (26.4°N, 38.5°W; 32.5°N, 30.0°W; 22.5°N, 28.5°W). *Jenkins* [1998] found similar oxygen consumption rates in the eastern subtropical North Atlantic. *Brea et al.* [2004] estimate a remineralization rates of 5.1 $\mu$mol $O_2$/kg/a for Antarctic Intermediate Water (~400–1000 m) in the Eastern South Atlantic. We expect the estimate of *Brea et al.* [2004] to be high because of increased rates of production and respiration in their study region resulting from the Benguela upwelling [*Chapman and Shannon*, 1987]. Since our estimated respiration rate is averaged over the entire basin, our estimate of 3.2 $\mu$mol $O_2$/kg/a is in reasonably good agreement with *Brea et al.* [2004].

[35] While the models are able to fit the observed $O_2$ data with realistic values of advection, diffusion, respiration, and respiratory fractionation, all model solutions that recreate the observed $\delta^{18}O$ to $O_2$ relationship require an end-member with an $[O_2]$ that is much lower and $\delta^{18}O$ value that is much higher than the observed values. Waters with these very low oxygen concentrations were not sampled during SAVE-2 and other South Atlantic cruises. A recent reanalysis of the Global Ocean Data Analysis Project (GLODAP) data set by *Karstensen et al.* [2008], shows minimum $[O_2]$ in the South Atlantic to be on the order of 17 $\mu$mol/kg (~6% of saturation using standard temperature and salinity values for the oxygen minimum region). They estimate from a comprehensive $O_2$ climatology that waters with less than 45 $\mu$mol/kg (~16% of saturation) make up ~1% of the South Atlantic volume. This is in contrast to the eastern Pacific where waters become suboxic (<4.5 $\mu$mol/kg) and where the oxygen minimum zone makes up ~20% of the North Pacific volume.

[36] There are three possible explanations of the model results: (1) large-scale hydrographic programs have missed small pockets of low-$O_2$ waters which have a significant effect on the oxygen isotopic signature, (2) the prediction of a low-$O_2$ end-member is a result of model limitations, and (3) the fractionation factor ($\alpha$) measured in the laboratory is not representative of the oceanic community. There are several possible sources of low-$O_2$, high-$\delta^{18}O$ waters. First, organisms may sink as aggregates, with high internal rates of $O_2$ consumption resulting in extremely low [$O_2$] or anoxic conditions in particle interiors. While this process undoubtedly contributes to the oxygen isotopic signature, very limited studies [*Ploug*, 2001; *Ploug et al.*, 2002] suggest that interior $O_2$ concentrations are not that low, and so respiration in aggregates does not have a dramatic effect on $\delta^{18}O$ of dissolved $O_2$ in the ocean. Second, similarly, sedimentary diagenesis, with extensive $O_2$ consumption near the sediment-water interface, may imprint overlying waters with the isotopic signature of low-$O_2$ waters [*Bender*, 1990]. However, the $O_2$ minimum lies in the depth interval of the thermocline where most $O_2$ utilization takes place in the water column rather than in the sediments.

[37] The 1-D and 2-D models presented here could require an unrealistic end-member in order to compensate for a simplified advection-diffusion geometry. The oxygen minimum zone sampled by the SAVE-2 transect occurs between the subequatorial and subtropical gyres and is believed to result from slow ventilation and increased respiration [*Chapman and Shannon*, 1987]. While the 2-D model attempts to capture this 'shadow zone' with the double gyre advection geometry, it is still a simplified view of the circulation in the South Atlantic. Specifically, there is no advective exchange between the two gyres. This results in an underestimate of the oxygen concentrations in the northern gyre and consequently a significantly larger oxygen minimum zone than is observed in the SAVE data. While the model overestimates the volume of low-oxygen waters present in the study region, model sensitivity studies (not shown) indicate that model results are robust and that mixing with a low-$O_2$ end-member is required to best match the observed $\delta^{18}O/[O_2]$ relationship.

[38] One can ask whether three dimensional water mass geometry may depress $\delta^{18}O$ of $O_2$ more than the vertical and isopycnal mixing in our idealized 1-D and 2-D experiments and allow for the observed $\delta^{18}O/[O_2]$ relationship without a low-$O_2$ end-member. While a three-dimensional model is beyond the scope of this paper, the $\delta^{18}O/[O_2]$ relationship from *Maier-Reimer*'s [1993] 3-D ocean biogeochemistry–general circulation model provides a point of comparison. Interestingly, Maier-Reimer's complex model produces some of the same features observed in our 2-D isopycnal slab model (Figure 4). Specifically, the 3-D model comes close to fitting *Kroopnick*'s [1987] Pacific data using $\alpha = 0.982$, but requires mixing with low [$O_2$] (<1% of saturation) and high $\delta^{18}O$ values (>32‰). Again, such low $O_2$ concentrations are not observed in most of the world's oceans. The similarity between Maier-Reimer's complex 3-D model and our 2-D model reinforces the results from our analysis.

[39] Finally, our 1-D and 2-D sensitivity analysis indicates that increases in the isotopic fractionation factor ($\alpha$) can depress the $\delta^{18}O/[O_2]$ relationship and allow the model to fit the observations without the low-oxygen end-member (Figure 4d, inset). This is also observed in the diapycnal analysis where the model requires an isotope effect that is significantly lower ($\alpha = 0.992$) than those measured in culture ($\alpha = 0.981$). Because of the fixed boundary conditions of the diapycnal model, the model $O_2$ concentrations never fall to the level required to simulate the observed values of $\delta^{18}O$ with the traditional fractionation factor. Therefore, the model is forced to use a higher $\alpha$ value in order to represent the observed $\delta^{18}O/[O_2]$ relationship. This presents the third possible explanation of the model results: $\alpha$ values measured in culture may not be representative of oceanic organisms. Supporting evidence for the laboratory values comes from estimates of the fractionation factors for the individual $O_2$ consumption pathways [*Guy et al.*, 1993; *Helman et al.*, 2005; *Kiddon et al.*, 1993] and the respiratory fractionation factor for mixed layer ecosystems [*Hendricks et al.*, 2005; *Quay et al.*, 1993]. Both range around the whole organism values measured in the laboratory. However, these values may still not be representative of fractionation factors present in low-$O_2$ communities. In addition, according to *Anderson and Sarmiento* [1994], 19% of $O_2$ consumption derives from the oxidation of $NH_4^+$ to $NO_3^-$. The fractionation factors associated with this reaction are currently unknown and so could increase the community oxygen fractionating factor if they are shown to be less fractionating than those of cytochrome oxidase and the other pathways of $O_2$ consumption. Finally, complete oxygen consumption in sinking particles or in the sediments ($\alpha = 1$) could impart a high apparent oxygen fractionation factor on the surrounding waters.

## 5. Conclusions

[40] $\delta^{18}O$ of dissolved $O_2$ is a useful tracer for studying mixing and respiration in the mesopelagic ocean. In this paper, we present data from the tropical South Atlantic thermocline including the intense $O_2$ minimum zone. These data complement a profile from the subtropical North Atlantic [*Kroopnick et al.*, 1972], the extensive Pacific GEOSECS study of *Kroopnick* [1987], and the subarctic Pacific thermocline data of *Quay et al.* [1993]. For all of the data sets, we find a monotonic relationship in well oxygenated waters (>40% of saturations) with increasing $\delta^{18}O$ of $O_2$ as $[O_2]/[O_2]_{saturation}$ decreases, indicating that similar relative patterns of isotopic fractionation, mixing and respiration exist throughout the global ocean. In oxygen poor waters (<40% of saturation), there is a deviation in the isotopic signature of up to 10‰ between the South Atlantic oxygen minimum waters and Pacific thermocline waters with the same saturation level. This deviation is attributed to variations in the relative rates of mixing and respiration experienced by the water masses and indicates that the $\delta^{18}O$ signature can be used to clarify the interaction of diffusion, advection and respiration in oxygen minimum zones.

[41] We use a suite of advection-reaction-diffusion models to evaluate the oxygen concentration and isotope data

from the SAVE-2 transect. Contrary to the findings of previous studies [*Bender*, 1990; *Quay et al.*, 1993], we conclude that the Peclet number along isopycnal surfaces is too high to allow the data to be described simply in terms of lateral diffusion and respiration. Advection is required to reproduce the linear $\delta^{18}O/[O_2]$ relationship in oxygenated waters (>40% saturation), while diffusion produces the curvature observed in low-$O_2$ waters. The respiration rates estimated using a 2-D isopycnal slab model and 1-D diapycnal model, 2.9 $\mu$mol $O_2$/kg/a and 0.31 $\mu$mol $O_2$/kg/a, respectively, are in rough agreement with previous estimates. It is important to note that diapycnal processes may play a significant role in determining tracer profiles particularly in regions with large vertical concentration gradients, such as oxygen minimum zones.

[42] The models consistently argue that the South Atlantic oxygen isotopic signature cannot be described using traditional oceanic processes and rates. Specifically, they require either minimum $[O_2]$ which have not been observed in the field or fractionation factors which are lower (higher $\alpha$) than have been measured in the laboratory. This result indicates that we are missing or misrepresenting an important process in the mesopelagic ocean, particularly in low-oxygen waters. A more comprehensive sampling of oxygen minimum zones, such as the Eastern Tropical Pacific, and Arabian Sea, would help elucidate the physical and biogeochemical processes occurring in these regions; important players in the global carbon cycle. Additional measurements will also help constrain the extent of anoxia and range of $\delta^{18}O$ values found in the mesopelagic ocean. Contemporaneous measurements with Lagrangian floats and transient tracers (CFCs, tritium-$^3$He) would refine estimates of circulation and ventilation [*Howell et al.*, 1997]. Finally, adding oxygen isotopes to a state-of-the-art model with a more realistic representation of 3-D circulation and biogeochemistry will allow us to investigate the importance and extent of low-$O_2$ waters in determining the oxygen isotopic signature and will ultimately lead to a better understanding of the interaction between transport and respiration that determines the distribution of tracers in the dark ocean.

[43] **Acknowledgments.** The authors would like to thank John A. Kiddon for collecting the samples analyzed in this paper, John P. Dunne for his help with the modeling effort, and Bruce Barnett for his tireless help in the laboratory. We gratefully acknowledge financial support from NSF and NASA. We would also like to acknowledge the helpful comments of anonymous reviewers.

## References

Anderson, L. A., and J. L. Sarmiento (1994), Redfield ratios of remineralization determined by nutrient data analysis, *Global Biogeochem. Cycles*, *8*, 65–80, doi:10.1029/93GB03318.

Bender, M. L. (1990), The $\delta^{18}O$ of dissolved $O_2$ in seawater: A unique tracer of circulation and respiration in the deep sea, *J. Geophys. Res.*, *95*, 22,243–22,252, doi:10.1029/JC095iC12p22243.

Bender, M., and K. D. Grande (1987), Production, respiration, and the isotope geochemistry of $O_2$ in the upper water column, *Global Biogeochem. Cycles*, *1*, 49–59, doi:10.1029/GB001i001p00049.

Brea, S., X. A. Álvarez-Salgado, M. Álvarez, F. F. Pérez, L. Mémery, H. Mercier, and M. J. Messias (2004), Nutrient mineralization rates and ratios in the eastern South Atlantic, *J. Geophys. Res.*, *109*, C05030, doi:10.1029/2003JC002051.

Broecker, W. S., S. Blanton, W. M. Smethie Jr., and G. Ostlund (1991), Radiocarbon decay and oxygen utilization in the deep Atlantic Ocean, *Global Biogeochem. Cycles*, *5*, 87–117, doi:10.1029/90GB02279.

Buesseler, K. O., et al. (2007), Revisiting carbon flux through the ocean's twilight zone, *Science*, *316*, 567–570, doi:10.1126/science.1137959.

Chapman, P., and L. V. Shannon (1987), Seasonality in the oxygen minimum layers at the extremities of the Benguela System, *S. Afr. J. Mar. Sci.*, *5*, 85–94.

Craig, H. (1969), Abyssal carbon and radiocarbon in the Pacific, *J. Geophys. Res.*, *74*, 5491–5506, doi:10.1029/JC074i023p05491.

Doney, S. C., W. J. Jenkins, and J. L. Bullister (1997), A comparison of ocean tracer dating techniques on a meridional section in the eastern North Atlantic, *Deep Sea Res., Part I*, *44*, 603–626, doi:10.1016/S0967-0637(96)00105-7.

Feely, R. A., C. L. Sabine, R. Schlitzer, J. L. Bullister, S. Mecking, and D. Greeley (2004), Oxygen utilization and organic carbon remineralization in the upper water column of the Pacific Ocean, *J. Oceanogr.*, *60*, 45–52, doi:10.1023/B:JOCE.0000038317.01279.aa.

Guy, R. D., J. A. Berry, M. L. Fogel, and T. C. Hoering (1989), Differential fractionation of oxygen isotopes by cyanide-resistant and cyanide-sensitive respiration in plants, *Planta*, *177*, 483–491, doi:10.1007/BF00392616.

Guy, R. D., M. L. Fogel, and J. A. Berry (1993), Photosynthetic fractionation of the stable isotopes of oxygen and carbon, *Plant Physiol.*, *101*, 37–47.

Haine, T. W. N., and T. M. Hall (2002), A generalized transport theory: Water-mass composition and age, *J. Phys. Oceanogr.*, *32*, 1932–1946, doi:10.1175/1520-0485(2002)032<1932:AGTTWM>2.0.CO;2.

Helman, Y., E. Barkan, D. Eisenstadt, B. Luz, and A. Kaplan (2005), Fractionation of the three stable oxygen isotopes by oxygen-producing and oxygen-consuming reactions in photosynthetic organisms, *Plant Physiol.*, *138*, 2292–2298, doi:10.1104/pp.105.063768.

Hendricks, M. B., M. L. Bender, B. A. Barnett, P. Strutton, and F. P. Chavez (2005), Triple oxygen isotope composition of dissolved $O_2$ in the equatorial Pacific: A tracer of mixing, production, and respiration, *J. Geophys. Res.*, *110*, C12021, doi:10.1029/2004JC002735.

Henning, C. C., D. Archer, and I. Fung (2006), Argon as a tracer of cross-isopycnal mixing in the thermocline, *J. Phys. Oceanogr.*, *36*, 2090–2105, doi:10.1175/JPO2961.1.

Howell, E. A., S. C. Doney, R. A. Fine, and D. B. Olson (1997), Geochemical estimates of denitrification in the Arabian Sea and the Bay of Bengal during WOCE, *Geophys. Res. Lett.*, *24*, 2549–2552, doi:10.1029/97GL01538.

Ito, T., and C. Deutsch (2006), Understanding the saturation state of argon in the thermocline: The role of air-sea gas exchange and diapycnal mixing, *Global Biogeochem. Cycles*, *20*, GB3019, doi:10.1029/2005GB002655.

Jenkins, W. J. (1982), Oxygen utilization rates in North Atlantic subtropical gyre and primary production in oligotrophic systems, *Nature*, *300*, 246–248, doi:10.1038/300246a0.

Jenkins, W. J. (1987), $^3H$ and $^3He$ in the Beta Triangle: Observations of gyre ventilation and oxygen utilization rates, *J. Phys. Oceanogr.*, *17*, 763–783, doi:10.1175/1520-0485(1987)017<0763:AITBTO>2.0.CO;2.

Jenkins, W. J. (1988), The use of anthropogenic tritium and Helium-3 to study subtropical gyre ventilation and circulation, *Philos. Trans. R. Soc. London, Ser. A*, *325*, 43–61, doi:10.1098/rsta.1988.0041.

Jenkins, W. J. (1998), Studying subtropical thermocline ventilation and circulation using tritium and $^3He$, *J. Geophys. Res.*, *103*, 15,817–15,831, doi:10.1029/98JC00141.

Karstensen, J., L. Stramma, and M. Visbeck (2008), Oxygen minimum zones in the eastern tropical Atlantic and Pacific oceans, *Prog. Oceanogr.*, *77*, 331–350, doi:10.1016/j.pocean.2007.05.009.

Key, R. M., P. D. Quay, P. Schlosser, A. P. McNichol, K. F. von Reden, R. J. Schneider, K. L. Elder, M. Stuiver, and H. G. Östlund (2002), WOCE radiocarbon IV: Pacific Ocean results; P10, P13N, P14C, P18, P19 & S4P, *Radiocarbon*, *44*, 239–392.

Kiddon, J. (1993), $O_2$ and $^{18}O$: Co-Tracers of Oceanic Productivity, Ph.D. thesis, 187 pp., Univ. of Rhode Island, Kingston, R. I.

Kiddon, J., M. L. Bender, J. Orchardo, D. A. Caron, J. C. Goldman, and M. Dennett (1993), Isotopic fractionation of oxygen by respiring marine organisms, *Global Biogeochem. Cycles*, *7*, 679–694, doi:10.1029/93GB01444.

Kroopnick, P. (1987), *Oxygen 18 in Dissolved Oxygen*, vol. 3, pp. 27–182, U.S. Gov. Print. Off, Washington, D. C.

Kroopnick, P., and H. Craig (1976), Oxygen isotope fractionation in dissolved oxygen in deep sea, *Earth Planet. Sci. Lett.*, *32*, 375–388, doi:10.1016/0012-821X(76)90078-9.

Kroopnick, P., R. F. Weiss, and H. Craig (1972), Total $CO_2$, $^{13}C$, and dissolved oxygen-$^{18}O$ at GEOSECS II in the North Atlantic, *Earth Planet. Sci. Lett.*, *16*, 103–110, doi:10.1016/0012-821X(72)90242-7.

Lane, G. A., and M. Dole (1956), Fractionation of oxygen isotopes during respiration, *Science*, *123*, 574–576, doi:10.1126/science.123.3197.574.

Ledwell, J. R., A. J. Watson, and C. S. Law (1993), Evidence for slow mixing across the pycnocline from an open-ocean tracer-release experiment, *Nature*, *364*, 701–703, doi:10.1038/364701a0.

Maier-Reimer, E. (1993), Geochemical cycles in an ocean general circulation model: Preindustrial tracer distributions, *Global Biogeochem. Cycles*, *7*, 645–677, doi:10.1029/93GB01355.

Martin, J. H., G. A. Knauer, D. M. Karl, and W. W. Broenkow (1987), VERTEX: Carbon cycling in the northeast Pacific, *Deep Sea Res., Part A*, *34*, 267–285, doi:10.1016/0198-0149(87)90086-0.

Najjar, R. G., J. L. Sarmiento, and J. R. Toggweiler (1992), Downward transport and fate of organic matter in the ocean: Simulations with a general circulation model, *Global Biogeochem. Cycles*, *6*, 45–76, doi:10.1029/91GB02718.

Ploug, H. (2001), Small-scale oxygen fluxes and remineralization in sinking aggregates, *Limnol. Oceanogr.*, *46*, 1624–1631.

Ploug, P., S. Hietanen, and J. Kuparinen (2002), Diffusion and advection within and around sinking, porous diatom aggregates, *Limnol. Oceanogr.*, *47*, 1129–1136.

Quay, P. D., S. Emerson, D. O. Wilbur, G. Stump, and M. Knox (1993), The $\delta^{18}O$ of dissolved $O_2$ in the surface waters of the subarctic Pacific: A tracer of biological productivity, *J. Geophys. Res.*, *98*, 8447–8458, doi:10.1029/92JC03017.

Riley, G. A. (1951), Oxygen, phosphate, and nitrate in the Atlantic ocean, *Bull. Bingham Oceanogr. Coll.*, *13*, 1–126.

Robbins, P. E., J. F. Price, W. B. Owens, and W. J. Jenkins (2000), The importance of lateral diffusion for the ventilation of the lower thermocline in the subtropical North Atlantic, *J. Phys. Oceanogr.*, *30*, 67–89, doi:10.1175/1520-0485(2000)030<0067:TIOLDF>2.0.CO;2.

Schlitzer, R. (2002), Carbon export fluxes in the Southern Ocean: Results from inverse modeling and comparison with satellite-based estimates, *Deep Sea Res.*, *49*, 1623–1644.

Schlitzer, R. (2004), Export production in the equatorial and North Pacific derived from dissolved oxygen, nutrient and carbon data, *J. Oceanogr.*, *60*, 53–62, doi:10.1023/B:JOCE.0000038318.38916.e6.

South Atlantic Ventilation Experiment (1992), *Chemical, Physical and CTD Data Report*, *Leg 1, Leg 2, Leg 3, ODF Publ. 231, SIO Ref. 92-9*, Ocean Data Facility, Scripps Inst. of Oceanogr., Univ. of Calif., San Diego, April.

Sowers, T., M. Bender, and D. Raynaud (1989), Elemental and isotopic composition of occluded $O_2$ and $N_2$ in polar ice, *J. Geophys. Res.*, *94*, 5137–5150, doi:10.1029/JD094iD04p05137.

Stramma, L., and M. England (1999), On the water masses and mean circulation of the South Atlantic Ocean, *J. Geophys. Res.*, *104*, 20,863–20,883, doi:10.1029/1999JC900139.

Weiss, R. F. (1970), The solubility of nitrogen, oxygen and argon in water and seawater, *Deep Sea Res.*, *17*, 721–735.

M. L. Bender, Department of Geosciences, Princeton University, M48 Guyot Hall, Washington Road, Princeton, NJ 08544, USA.

S. C. Doney, Department of Marine Chemistry and Geochemistry, Woods Hole Oceanographic Institution, MS 25, 266 Woods Hole Road, Woods Hole, MA 02543, USA.

N. M. Levine, MIT-WHOI Joint Program, MS 25, 266 Woods Hole Road, Woods Hole, MA 02543, USA. (nlevine@whoi.edu)